**Supporting Information**

# Methylbismuth: An Organometallic Bismuthinidene Biradical

Deb Pratim Mukhopadhyay,[a] Domenik Schleier,[a] Sara Wirsing,[a] Jacqueline Ramler,[b] Dustin Kaiser,[a] Engelbert Reusch,[a] Patrick Hemberger,[c] Tobias Preitschopf,[a] Ivo Krummenacher,[b] Bernd Engels,*[a] Ingo Fischer,*[a] and Crispin Lichtenberg*[b]


[a]     Dr. Deb Pratim Mukhopadhyay, Domenik Schleier, Sara Wirsing, Dustin Kaiser, Engelbert Reusch, Tobias Preitschopf, Prof. Dr. Bernd Engels, Prof. Dr. Ingo Fischer
        Institut für Physikalische und Theoretische Chemie
        Universität Würzburg
        Am Hubland, D-97074 Würzburg
        E-mail: ingo.fischer@uni-wuerzburg.de, bernd.engels@uni-wuerzburg.de

[b]     Jacqueline Ramler, Dr. Ivo Krummenacher, Priv.-Doz. Dr. Crispin Lichtenberg
        Institut für Anorganische Chemie
        Universität Würzburg
        Am Hubland, D-97074 Würzburg.
        E-mail: crispin.lichtenberg@uni-wuerzburg.de

[c]     Dr. Patrick Hemberger
        Laboratory for Femtochemistry and Synchrotron Radiation
        Paul Scherrer Institut (PSI)
        CH-5232 Villigen, Switzerland.


**ORCID-identifiers**

Deb Pratim Mukhopadhyay:      https://orcid.org/0000-0002-2759-1934
Patrick Hemberger:            http://orcid.org/0000-0002-1251-4549
Bernd Engels:                 http://orcid.org/0000-0003-3057-389X
Ingo Fischer:                 http://orcid.org/0000-0001-8978-4013
Crispin Lichtenberg:          http://orcid.org/0000-0002-0176-0939

**Table of contents**

# Synthetic procedures and characterization of compound 8

**General considerations.** All air- and moisture-sensitive manipulations were carried out using standard vacuum line Schlenk techniques or in gloveboxes containing an atmosphere of purified argon. Solvents were degassed and purified according to standard laboratory procedures. NMR spectra were recorded on Bruker instruments operating 500 MHz with respect to $^1$H. $^1$H and $^{13}$C NMR chemical shifts are reported relative to SiMe$_4$ using the residual $^1$H and $^{13}$C chemical shifts of the solvent as a secondary standard. NMR spectra were recorded at ambient temperature (typically 25 °C). Single crystals suitable for X-ray diffraction were coated with polyisobutylene or perfluorinated polyether oil in a glovebox, transferred to a nylon loop and then transferred to the goniometer of a diffractometer equipped with a molybdenum X-ray tube ($\lambda = 0.71073$ Å). The structures were solved using intrinsic phasing methods (SHELXT) completed by Fourier synthesis and refined by full-matrix least-squares procedures. CCDC 1991253 contains the crystallographic information for this work. EPR spectra at X-band (9.4 GHz) were measured at room temperature on a Bruker ELEXSYS E580 EPR spectrometer, using 0.4 mW microwave power and 0.5 G field modulation at 100 kHz. The spectral simulations were performed using MATLAB 8.6 and the EasySpin 5.2.11 toolbox.[1]

**BiMe$_3$ (1).** Route A. The literature-known protocol[2] for the synthesis of BiMe$_3$ was improved. To a suspension of BiCl$_3$ (9.42 g, 29.9 mmol) in diethyl ether (150 mL) was added methylmagnesium bromide (3 M in Et$_2$O, 89.6 mmol, 29.8 mL) at 0 °C. The reaction mixture was stirred at 0 °C for 15 min, then 1.5 h at ambient temperature. The suspension was filtered, and diethyl ether was distilled at 55 °C. The residue was distilled at 90 °C and 5 x 10$^{-3}$ mbar to give the product as a colorless oil. Yield: 4.10 g, 15.0 mmol, 50%, 0.25 eq. Et$_2$O.

Route B:[2] To a suspension of magnesium turnings (3.23 g, 133 mmol) in diethyl ether (15 mL) was added a solution of MeI (17.8 g, 125 mmol) in diethyl ether (60 mL) dropwise at ambient temperature. The reaction mixture was stirred at ambient temperature for 1 h. The suspension was filtered, and the solution was added to a suspension of BiCl$_3$ (13.2 g, 41.9 mmol) in diethyl ether (250 mL) at 0 °C. The reaction mixture was stirred for 1 h at ambient temperature. All volatiles were removed under reduced pressure at 0 °C, and the residue was filtered and distilled at 130 °C to give BiMe$_3$ as a colorless oil. Yield: 1.01 g, 2.97 mmol, 7%, 1.16 eq. Et$_2$O.

The product can be obtained free of Et$_2$O by increasing the time during which Et$_2$O is distilled off at 55 °C, which leads to lower yields of **1**.

**Solid state structure of compound 8.** Compound **8** forms a one-dimensional coordination polymer in the solid state, which expands through translation along the crystallographic a-axis (Figure S1). The contact between neighboring monomeric subunits, BiMe(SPh)$_2$, is established via the sulfur atoms S1 and S2, which adopt bridging coordination modes between two bismuth atoms, Bi1 and Bi1'. The Bi–S1/2 bonds in a monomeric subunit (2.70-2.74 Å) are somewhat shorter than the Bi1–S1'/2' bonds linking these units (2.97-3.01 Å). The Bi1–C1 bond length of 2.21 Å is within limits of error identical to those in BiMe$_3$.[3] The bismuth atom of **8** is found in a square pyramidal coordination geometry with the carbon atom in the apical position ($\tau_5 = 0.02$).

A small number of related compounds BiR(SR')$_2$ have been reported in the literature (R = aryl, R' = aryl, alkyl).[4-7] However, no species with R = alkyl are known. Known species with R = aryl contain additional donor functional groups at the aryl substituent or additional donor ligands. This prevents a polymeric arrangement in the solid state for the literature-known species, making compound **8** the first coordination polymer of the type [BiR(SR')$_2$]$_\infty$ with sulfur atoms in the bridging positions.[8]
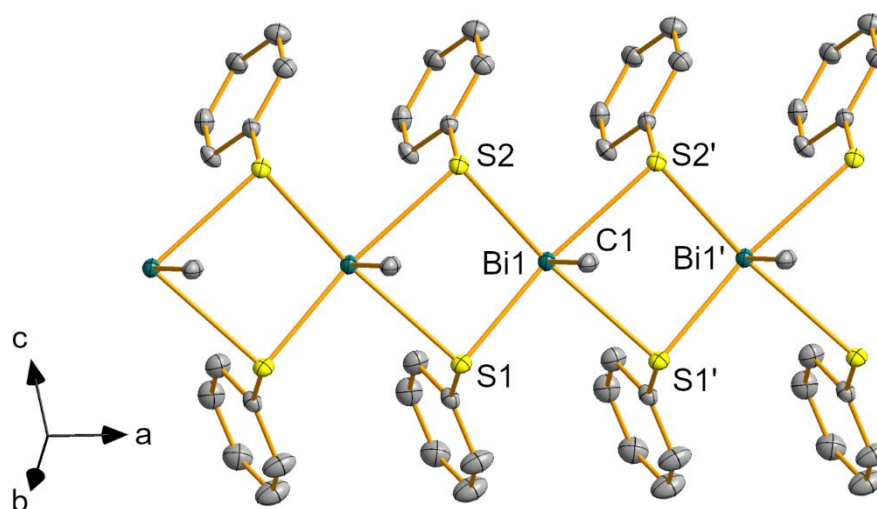


**Figure S1.** Arrangement of BiMe(SPh)$_2$ (**8**) as a one-dimensional coordination polymer in the solid state. Displacement ellipsoids are shown at the 50% probability level. Hydrogen atoms and one split position of disordered atoms are omitted for clarity. Selected bond lengths (Å) and angles (°): Bi1−C1, 2.208(10); Bi1−S1, 2.736(2); Bi1−S2, 2.699(2); Bi1'−S1, 3.014(2); Bi1'−S2, 2.970(2); C1−Bi1−S1, 89.6(3); C1−Bi1−S2, 89.4(3); S1−Bi1−S2, 93.18(7); S1−Bi1−S2', 170.05(7); S1'−Bi1−S2', 82.57(7); Bi1−S1'−Bi1', 90.75(7); Bi1−S2'−Bi1', 92.43(7).

# NMR spectra of compound 8
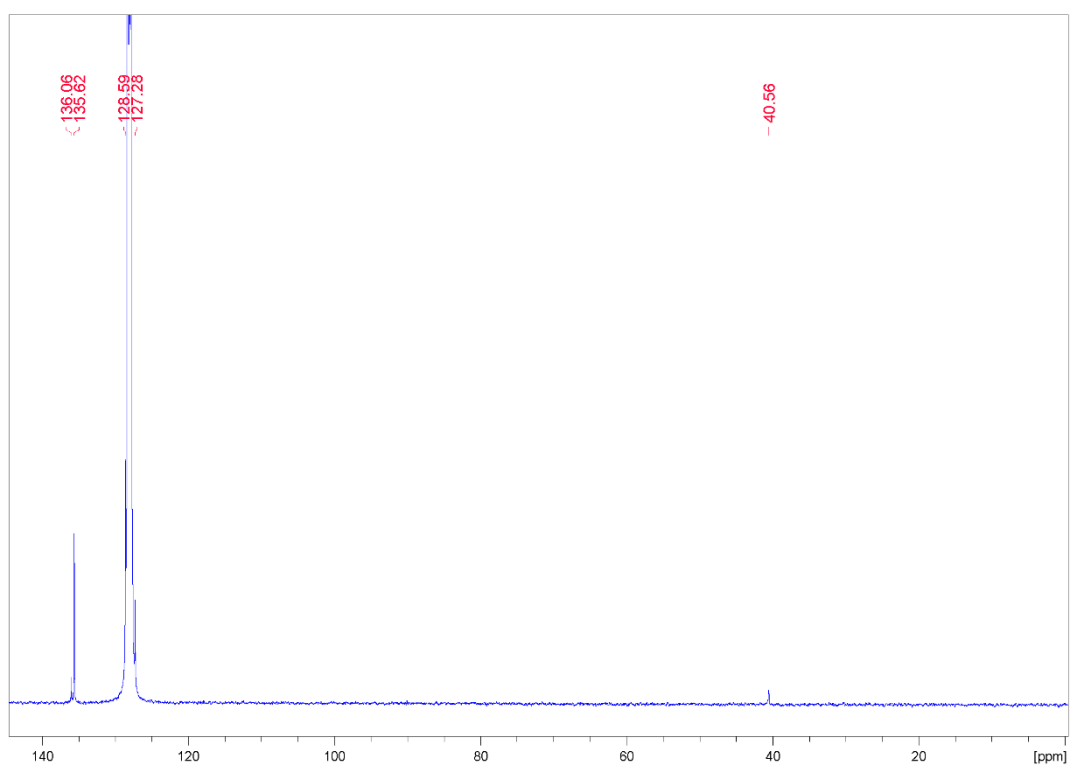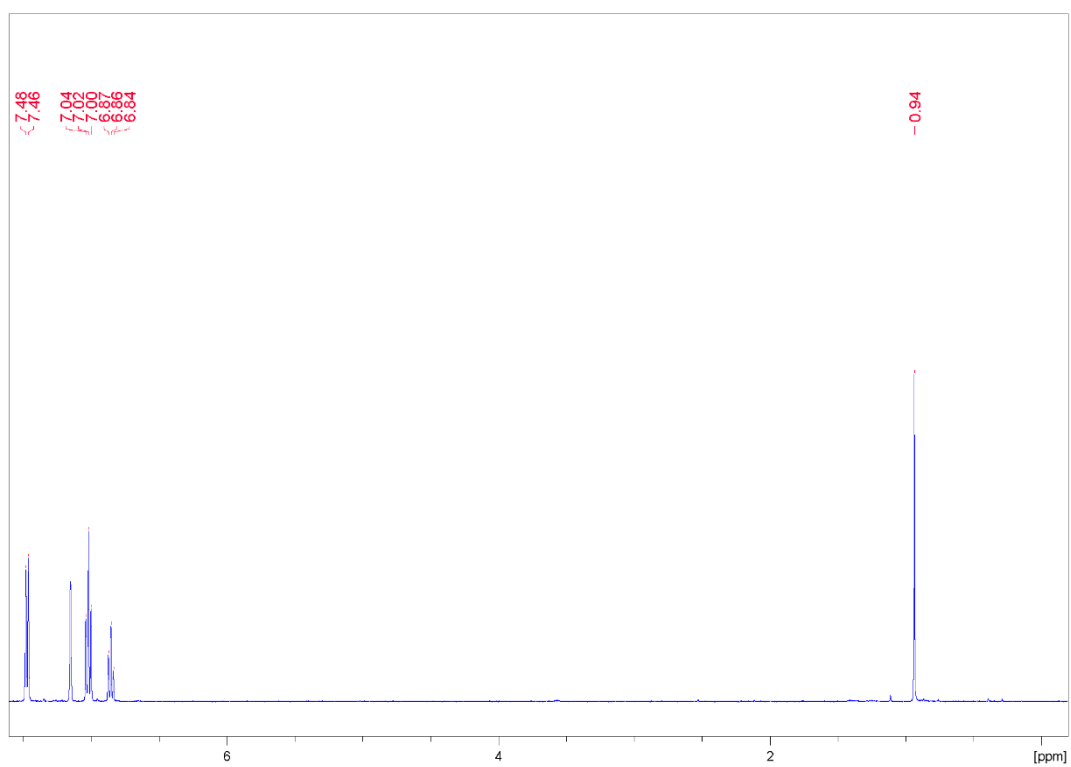


**Figure S2**. $^{1}$H and $^{13}$C NMR spectra of BiMe(SPh)$_2$ (**8**) in C$_6$D$_6$.

# Experimental methods for experiments with synchrotron radiation

The spectroscopic experiments were carried out at the VUV beamline of the Swiss Light Source (SLS) at the Paul-Scherrer Institute, Villigen/CH. Synchrotron radiation is provided by a bending magnet, collimated and diffracted by a plane grating (150 grooves·mm$^{-1}$) with a photon energy resolution of $1.5 \times 10^3$. Higher harmonic radiation was suppressed in a $MgF_2$ window. In most experiments the photon energy was scanned in 5 meV steps and calibrated using autoionization resonances in Ar. The ionization energies reported in the main paper are accurate to within ±20 meV and were corrected for the Stark-shift by the extraction field (8-9 meV). Note that in some experiments 10 meV steps were used. A detailed description of the beamline is given in the literature.[9] Experiments were carried out in a free jet apparatus equipped with a time-of-flight mass spectrometer and a velocity map imaging photoelectron spectrometer.[10] Ions and electrons were collected in coincidence, permitting to record ion mass-selected photoelectron spectra. Threshold electrons were selected with an energy resolution of 3-5 meV and the contribution of background electrons was subtracted. Precursor **1** was seeded in Ar and expanded through a 100 μm orifice into an electrically heated SiC tube based on an earlier design.[11]

# Computational Methods

In the computations, the geometries were optimized using the ORCA 4.1.1[12,13] package, employing the scalar relativistic ZORA[14] variant of the ωB97X-D3[15,16] functional. The ZORA-def2-TZVP[17] basis set was used for carbon and hydrogen, the SARC-ZORA-TZVP[17] basis set for bismuth. The SARC-ZORA basis set allows for an all-electron treatment of heavy elements such as Bi in a computationally efficient manner with contractions optimized for the ZORA Hamiltonian. Vibrational frequencies were obtained in the same computations. The electronic energies and the ionization potentials were then calculated either with the same method or with the ORCA 4.2.[12,13] program package, employing state-specific NEVPT2[18-20] optimizations and the scalar-relativistic ZORA variant (see Tables S2-S17). ωB97X-D3 geometries and relative energies were also benchmarked with NEVPT2 calculations for selected compounds (Table S2 to S17). The same basis sets as in the DFT geometry optimization were used. For BiMe, a CAS space of (4,4) (neutral)/(3,4) (cation) was defined, for $BiMe_2$ (5,5) and (4,5) respectively. The spectra were simulated based on the DFT computations using ezSpectrum.[21] The calculation of the isodesmic reaction values is based on DFT calculations and the experimental values for the C–H bond dissociation in $CH_4$ taken from the literature.[25] Energies determined by theoretical methods reflect electronic energies of the molecules. For DFT calculations, the zero-point energy (ZPE) corrections were added. For the NEVPT2 calculations this was not possible, since the calculations of the ZPE correction requires full frequency calculations.

# Simulated ms-TPE spectrum of compound 5
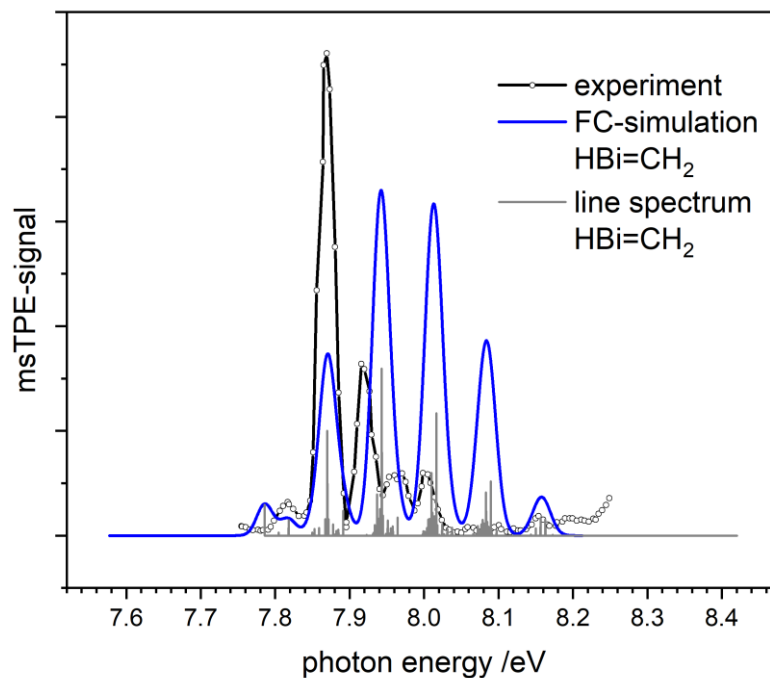


**Figure S3:** Comparison of the mass-selected threshold photoelectron spectrum of m/z=224 with the simulation based on the computations for $HBi=CH_2$, **5** (blue line). As visible, a strong vibrational progression is expected for **5**, the molecule can thus be ruled out as the carrier of the spectrum. Furthermore, it should be noted that C–H bond cleavage would be necessary for the formation of **5** (e.g.: $BDE(H_3C–H) = 439$ kJ·mol$^{-1}$)[25] and that further Bi–C bond cleavage (e.g.: $BDE(Me_2Bi–CH_3) = 210$ kJ·mol$^{-1}$ as determined in this study; lower Bi–C BDEs are expected for **2** and **3**) can be expected to be energetically favored.

# ms-TPE spectrum of Bi$_2$ with simulation
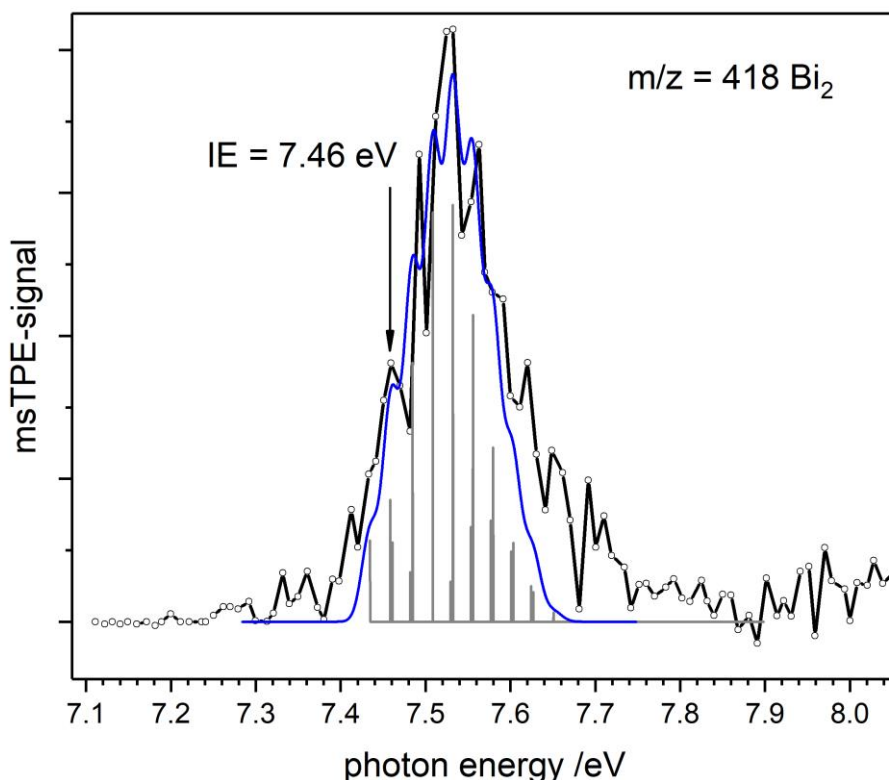


**Figure S4**: The $X^+$ $^2\Pi_{u3/2} \neg X$ $^1\Sigma_g^+$ photoionization transition of Bi$_2$ was also observed in the experiments. The ms-TPE spectrum appears to be slightly better resolved than the previously reported He(I) spectra.[22,23] The spectrum (solid line) was obtained by 5-point smoothing of the experimental data (open circles). Each data point (step size 10 meV) was averaged for 60 s. The solid blue line represents a Franck-Condon simulation based on the computed stick spectrum. Hot- and sequence bands contribute to the transition. As visible, the agreement between experiment and simulation is very good. An ionization energy of 7.46 eV is derived, which agrees well with the value of 7.44 eV reported by Wang et al..[23] The computations yielded $\tilde{\nu}^+ = 198$ cm$^{-1}$ and $\tilde{\nu}'' = 220$ cm$^{-1}$, in agreement with a reduction of bond length upon ionization from $R_e'' = 2.588$ Å to $R_e^+ = 2.686$ Å. Note that experimental values of $R_0'' = 2.66$ Å and $\tilde{\nu}'' = 172.21$ cm$^{-1}$ have been reported.[24] The bond order decreases, because an electron is removed from a $(\pi_u)^4$ bonding molecular orbital.

# IR spectrum of CH₄, detected in the reaction given in Figure 5
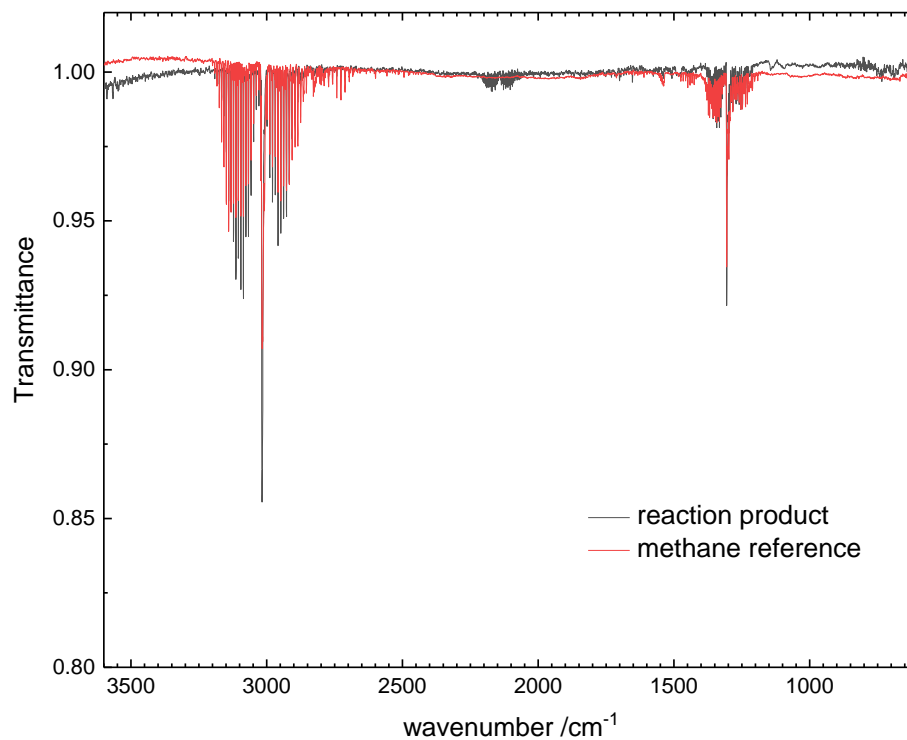


**Figure S5:** BiMe$_3$ was reacted with stoichiometric amounts of (PhS)$_2$ at 120 °C (see Figure 5 of main part). BiMe(SPh)$_2$ was isolated as a product of this reaction in 41% yield and fully characterized (see Figures 5, S1 and S2). As visible in the Figure, methane was detected in the headspace of the reaction by IR spectroscopy. This hints at the generation of methyl radicals, which produce methane through the abstraction of hydrogen atoms e.g. from the surface of the glassware. The spectrum was recorded on a Bruker IFS120HR spectrometer.

**Table S1.** Energies of the neutral ground states (relative to the energy of the lowest-energy-isomer **3**) along with experimental and calculated adiabatic IEs of all molecules investigated in this work. Zero point energy corrections are included in DFT calculations. If not stated otherwise all geometries are optimized with the same method that was used to determine the energy; energies are calculated with the one-center approximation.

| | **2** | **3** [a] | **4** [b] | **5** | **Bi$_2$** |
|---|---|---|---|---|---|
| Rel. energy /eV (DFT) | | 0.0 | +0.77 | +0.88 | |
| Rel. energy /eV (NEVPT2) | | 0.0 | +0.78 | +0.91[c] | |
| IE$_{calc}$ /eV (DFT) | 7.20 | 7.65 | 6.88 | 8.25 | 7.93 |
| IE$_{calc}$ /eV (NEVPT2) | 7.35 | 7.98 | 7.21 | 8.68[c] | 7.84 |
| IE$_{exp}$ /eV | 7.27 | 7.88 | | | 7.46 |

[a] triplet; [b] singlet; [c] determined from single-point NEVPT2 calculations on CASSCF (**3**) or DFT optimized geometries (**5** and **5**[•+]) without one-center approximation.

# Computed geometries and energies

# of 1, 2, 3, 4, 5, Bi₂ and their respective cations

**Table S2.** Geometry parameters of **1 (singlet)** and **1•+ (doublet)** computed by scalar-relativistic DFT in the ZORA variant with the ωB97X-D functional as described in the computational details section. Geometries were optimized without symmetry constraints.



| bond length (R) in Å | | | angle (A) in ° | | | dihedral (D) in ° | | |
|---|---|---|---|---|---|---|---|---|
| | neutral | cationic | | neutral | cationic | | neutral | cationic |
| R(1,2) | 2.250 | 2.222 | | | | | | |
| R(3,2) | 1.090 | 1.086 | A(3,2,1) | 109.7 | 108.8 | | | |
| R(4,2) | 1.089 | 1.091 | A(4,2,1) | 109.6 | 105.4 | D(4,2,1,3) | 239.8 | 240.7 |
| R(5,2) | 1.090 | 1.086 | A(5,2,1) | 109.7 | 108.5 | D(5,2,1,3) | 119.6 | 121.3 |
| R(1,6) | 2.250 | 2.222 | A(6,1,2) | 93.5 | 107.1 | D(6,1,2,3) | 73.2 | 67.0 |
| R(7,6) | 1.090 | 1.087 | A(7,6,1) | 109.7 | 108.7 | D(7,6,1,2) | 287.0 | 302.5 |
| R(8,6) | 1.089 | 1.091 | A(8,6,1) | 109.6 | 105.4 | D(8,6,1,2) | 47.2 | 61.9 |
| R(9,6) | 1.090 | 1.086 | A(9,6,1) | 109.7 | 108.7 | D(9,6,1,2) | 167.4 | 181.1 |
| R(1,10) | 2.250 | 2.222 | A(10,1,2) | 93.5 | 107.0 | D(10,1,2,3) | 167.0 | 181.2 |
| R(11,10) | 1.089 | 1.091 | A(11,10,1) | 109.6 | 105.4 | D(11,10,1,2) | 313.3 | 301.3 |
| R(12,10) | 1.090 | 1.086 | A(12,10,1) | 109.7 | 108.7 | D(12,10,1,2) | 73.5 | 60.7 |
| R(13,10) | 1.090 | 1.086 | A(13,10,1) | 109.7 | 108.7 | D(13,10,1,2) | 193.0 | 182.1 |

**Table S3.** Energies of **1** (singlet) and **1•+** (doublet) computed by scalar-relativistic DFT in the ZORA variant with the ωB97X-D functional as described in the computational details section. Energies are calculated with the one-center approximation and zero-point-energy correction on optimized geometries.

| | neutral (singlet) | neutral (triplet)[a] | cationic |
|---|---|---|---|
| Energy (Hartree) | –22509.381 | –22509.298 | –22509.084 |
| ΔE in eV | 0.00 | 2.24 | 8.07 |

[a] one imaginary frequency of –27.40 cm⁻¹.

**Table S4.** Geometry parameters of **2** (doublet) and **2⁺** (singlet) computed by scalar-relativistic DFT in the ZORA variant with the ωB97X-D functional as described in the computational details section. Geometries were optimized without symmetry constraints.
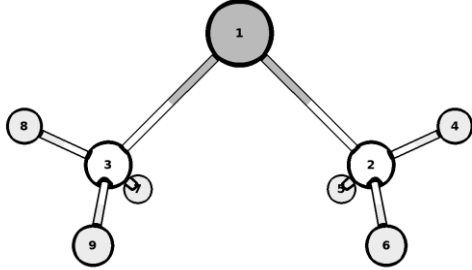


| bond length (R) in Å | | | angle (A) in ° | | | dihedral (D) in ° | | |
|---|---|---|---|---|---|---|---|---|
| | neutral | cationic | | neutral | cationic | | neutral | cationic |
| R(1,2) | 2.252 | 2.200 | | | | | | |
| R(1,3) | 2.252 | 2.200 | A(3,1,2) | 92.6 | 94.4 | | | |
| R(4,2) | 1.089 | 1.087 | A(4,2,1) | 110.0 | 111.1 | D(4,2,1,3) | 180.0 | 166.4 |
| R(5,2) | 1.090 | 1.090 | A(5,2,1) | 109.5 | 109.8 | D(5,2,1,3) | 59.8 | 42.8 |
| R(6,2) | 1.090 | 1.095 | A(6,2,1) | 109.5 | 106.7 | D(6,2,1,3) | 300.2 | 285.9 |
| R(7,3) | 1.090 | 1.095 | A(7,3,1) | 109.6 | 106.7 | D(7,3,1,2) | 300.3 | 285.7 |
| R(8,3) | 1.089 | 1.087 | A(8,3,1) | 110.0 | 111.0 | D(8,3,1,2) | 180.1 | 166.3 |
| R(9,3) | 1.090 | 1.090 | A(9,3,1) | 109.5 | 109.8 | D(9,3,1,2) | 59.8 | 42.7 |

**Table S5.** Energies of **2** (doublet) and **2⁺** (singlet) computed by scalar-relativistic DFT in the ZORA variant with the ωB97X-D functional as described in the computational details section. Energies are calculated with the one-center approximation and zero-point-energy correction on optimized geometries.

| | neutral | cationic (singlet) | cationic (triplet) |
|---|---|---|---|
| Energy (Hartree) | −22469.462 | −22469.198 | −22469.143 |
| ΔE in eV | 0.00 | 7.20 | 8.69 |

**Table S6.** Geometry parameters of **2** (doublet) and **2**⁺ (singlet) computed by NEVPT2 in the ZORA variant as described in the computational details section. Geometries were optimized without symmetry constraints.



| bond length (R) in Å | | | angle (A) in ° | | | dihedral (D) in ° | | |
|---|---|---|---|---|---|---|---|---|
| | neutral | cationic | | neutral | cationic | | neutral | cationic |
| R(1,2) | 2.267 | 2.213 | | | | | | |
| R(1,3) | 2.268 | 2.213 | A(3,1,2) | 90.9 | 92.6 | | | |
| R(4,2) | 1.089 | 1.087 | A(4,2,1) | 109.8 | 111.2 | D(4,2,1,3) | 185.9 | 167.0 |
| R(5,2) | 1.089 | 1.091 | A(5,2,1) | 109.1 | 108.8 | D(5,2,1,3) | 65.3 | 43.4 |
| R(6,2) | 1.090 | 1.095 | A(6,2,1) | 109.8 | 105.9 | D(6,2,1,3) | 305.9 | 286.7 |
| R(7,3) | 1.089 | 1.096 | A(7,3,1) | 109.1 | 105.1 | D(7,3,1,2) | 295.8 | 276.1 |
| R(8,3) | 1.088 | 1.088 | A(8,3,1) | 109.9 | 110.9 | D(8,3,1,2) | 174.5 | 157.9 |
| R(9,3) | 1.090 | 1.089 | A(9,3,1) | 108.7 | 109.8 | D(9,3,1,2) | 54.5 | 33.4 |

**Table S7.** Energies of **2** (doublet) and **2**⁺ (singlet) computed by NEVPT2 in the ZORA variant as described in the computational details section. Energies are calculated with the one-center approximation on optimized geometries.

| | neutral | cationic (singlet) |
|---|---|---|
| Energy (Hartree) | –22463.690 | –22463.420 |
| ΔE in eV | 0.00 | 7.35 |

**Table S8.** Geometry parameters of **3** (triplet bismuthinidene) and **3•+** (doublet) computed by scalar-relativistic DFT in the ZORA variant with the ωB97X-D functional as described in the computational details section. Geometries were optimized without symmetry constraints.
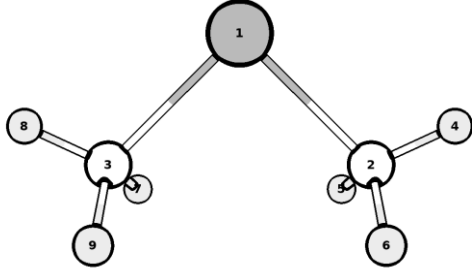


| bond length (R) in Å | | | angle (A) in ° | | | dihedral (D) in ° | | |
|---|---|---|---|---|---|---|---|---|
| | neutral | cationic | | neutral | cationic | | neutral | cationic |
| R(1,2) | 2.253 | 2.190 | | | | | | |
| R(3,2) | 1.089 | 1.089 | A(3,2,1) | 109.7 | 111.0 | | | |
| R(4,2) | 1.089 | 1.090 | A(4,2,1) | 109.7 | 110.5 | D(4,2,1,3) | 240.0 | 235.7 |
| R(5,2) | 1.089 | 1.097 | A(5,2,1) | 109.7 | 106.0 | D(5,2,1,3) | 120.0 | 118.2 |

**Table S9.** Energies of **3** (triplet bismuthinidene) and **3•+** (doublet) computed by scalar-relativistic DFT in the ZORA variant with the ωB97X-D functional as described in the computational details section. Energies are calculated with the one-center approximation and zero-point-energy correction on optimized geometries.

| | neutral | cationic |
|---|---|---|
| Energy (Hartree) | −22429.548 | −22429.267 |
| ΔE in eV | 0.00 | 7.65 |

**Table S10.** Geometry parameters of **3** (triplet bismuthinidene) and **3•+** (doublet) computed by NEVPT2 in the ZORA variant as described in the computational details section. Geometries were optimized without symmetry constraints.
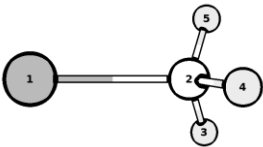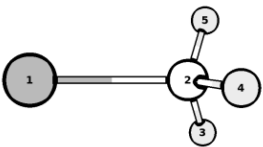


| bond length (R) in Å | | | angle (A) in ° | | | dihedral (D) in ° | | |
|---|---|---|---|---|---|---|---|---|
| | neutral | cationic | | neutral | cationic | | neutral | cationic |
| R(1,2) | 2.272 | 2.205 | | | | | | |
| R(3,2) | 1.089 | 1.089 | A(3,2,1) | 109.5 | 110.5 | | | |
| R(4,2) | 1.088 | 1.089 | A(4,2,1) | 108.7 | 110.4 | D(4,2,1,3) | 239.9 | 235.6 |
| R(5,2) | 1.088 | 1.097 | A(5,2,1) | 108.7 | 105.0 | D(5,2,1,3) | 120.0 | 117.8 |

**Table S11.** Energies of **3** (triplet bismuthinidene) and **3•+** (doublet) computed by NEVPT2 in the ZORA variant as described in the computational details section. Energies are calculated with the one-center approximation on optimized geometries.

| | neutral | cationic |
|---|---|---|
| Energy (Hartree) | −22423.859 | −22423.565 |
| ΔE in eV | 0.00 | 7.98 |

**Table S12.** Geometry parameters of **4** (closed shell singlet) computed as described in the computational details section. Geometries were optimized without symmetry constraints for the lowest singlet state.



| bond length (R) in Å | | | angle (A) in ° | | | dihedral (D) in ° | | |
|---|---|---|---|---|---|---|---|---|
| | DFT | NEVPT2 | | DFT | NEVPT2 | | DFT | NEVPT2 |
| R(1,2) | 2.244 | 2.267 | | | | | | |
| R(3,2) | 1.096 | 1.089 | A(3,2,1) | 103.8 | 109.3 | | | |
| R(4,2) | 1.087 | 1.089 | A(4,2,1) | 112.6 | 109.1 | D(4,2,1,3) | 243.4 | 240.1 |
| R(5,2) | 1.087 | 1.089 | A(5,2,1) | 112.5 | 109.3 | D(5,2,1,3) | 116.4 | 120.2 |

DFT converges to a CS configuration, NEVPT2 to a degenerate combination of states. Both methods find the first singlet root to be located ~0.8 eV above the triplet root when optimized.

**Table S13.** Energies of **4** (singlet) computed for comparison with **3** as described in the computational details section. Energies are calculated with the one-center approximation on optimized geometries, the DFT energy is zero-point-energy corrected.

| | DFT | NEVPT2 |
|---|---|---|
| Energy (Hartree) | –22429.519 | –22423.830 |

**Table S14.** Geometry parameters of **5** (singlet) and **5$^+$** (doublet) computed by scalar-relativistic DFT in the ZORA variant with the ωB97X-D functional as described in the computational details section. Geometries were optimized without symmetry constraints.



| bond length (R) in Å | | | angle (A) in ° | | | dihedral (D) in ° | | |
|---|---|---|---|---|---|---|---|---|
| | neutral | cationic | | neutral | cationic | | neutral | cationic |
| R(1,2) | 2.040 | 2.159 | | | | | | |
| R(3,2) | 1.082 | 1.085 | A(3,2,1) | 123.9 | 122.9 | | | |
| R(4,2) | 1.085 | 1.086 | A(4,2,1) | 120.4 | 120.8 | D(4,2,1,3) | 180.0 | 180.0 |
| R(5,1) | 1.795 | 1.781 | A(5,1,2) | 94.1 | 91.7 | D(5,1,2,3) | 359.9 | 359.9 |

**Table S15.** Energies of **5** (singlet) and **5$^{\bullet+}$** (doublet) computed by scalar-relativistic DFT in the ZORA variant with the ωB97X-D functional as described in the computational details section. Energies are calculated with the one-center approximation and zero-point-energy correction on optimized geometries.

| | neutral | cationic |
|---|---|---|
| Energy (Hartree) | –22429.515 | –22429.212 |
| ΔE in eV | 0.00 | 8.25 |

**Table S16.** Geometry parameters and energies of $Bi_2$ and $Bi_2^{\bullet+}$ computed by scalar-relativistic DFT in the ZORA variant with the ωB97X-D functional as described in the computational details section. Geometries were optimized without symmetry constraints. Energies are calculated with the one-center approximation and zero-point-energy corrected.
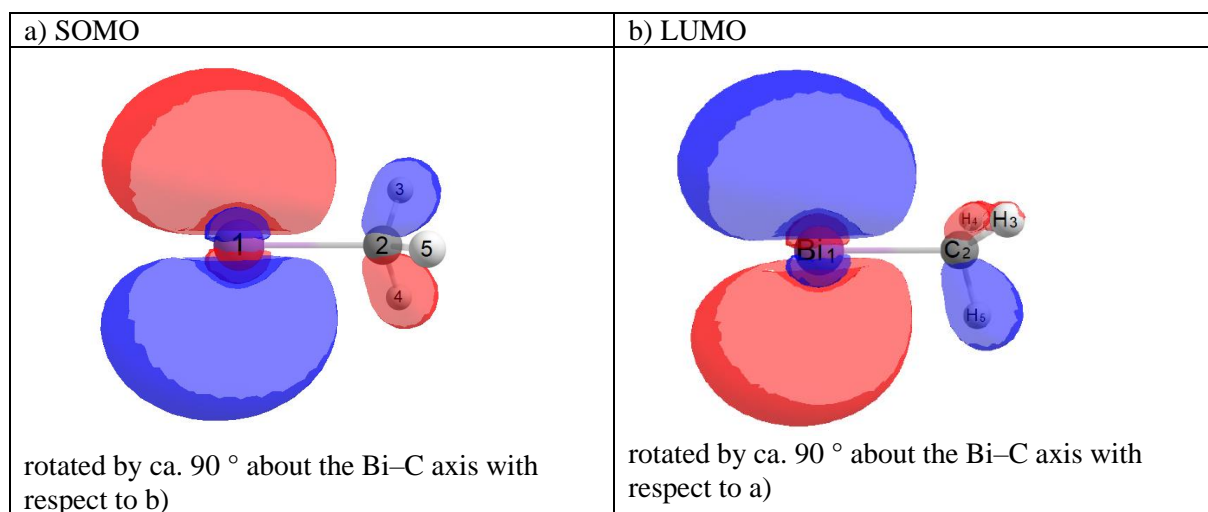
| bond length (R) in Å | | energy in Hartree | ΔE in eV |
|---|---|---|---|
| | neutral | cationic | | |
| singlet | 2.588 | | –44779.381 | 0 |
| triplet | 2.781 | | –44779.325 | 1.55 |
| doublet | | 2.686 | –44779.090 | 7.93 |

**Table S17.** Geometry parameters and energies of $Bi_2$ and $Bi_2^{\bullet+}$ computed by NEVPT2 in the ZORA variant as described in the computational details section with a CAS space of (6,6) for the neutral species and (5,6) for the cation. Energies are calculated with the one-center approximation on optimized geometries.

| bond length (R) in Å | | energy in Hartree | ΔE in eV |
|---|---|---|---|
| | neutral | cationic | | |
| singlet | 2.634 | | –44768.155 | 0 |
| doublet | | 2.745 | –44767.867 | 7.84 |

# Frontier Orbitals of 3$^{\bullet+}$

**Table S18.** Frontier orbitals of **3**$^{\bullet+}$ (doublet) computed by scalar-relativistic DFT in the ZORA variant with the ωB97X-D functional as described in the computational details section. The orbitals are shown at iso-values of 0.03. The molecules in the graphic representation of the SOMO and the LUMO are related to each other by a rotation of ca. 90° about the Bi–C axis in order to better visualize the respective orbitals.

| a) SOMO | b) LUMO |
|---|---|
|  |  |
| rotated by ca. 90 ° about the Bi–C axis with respect to b) | rotated by ca. 90 ° about the Bi–C axis with respect to a) |

**References**

1. S. Stoll and A. Schweiger, *J. Magn. Reson.*, 2006, **178**, 42-55.
2. K. Schäfer and F. Hein, *Z. Anorg. Allg. Chem.*, 1917, **100**, 249-303.
3. S. Schulz, A. Kuczkowski, D. Blaser, C. Wolper, G. Jansen and R. Haack, *Organometallics*, 2013, **32**, 5445-5450.
4. M. Dräger and B. M. Schmidt, *J. Organomet. Chem.*, 1985, **290**, 133-145.
5. P. Šimon, R. Jambor, A. Růžička and L. Dostál, *Organometallics*, 2013, **32**, 239-248.
6. K. M. Anderson, C. J. Baylies, A. H. M. Monowar Jahan, N. C. Norman, A. G. Orpen and J. Starbuck, *Dalton Trans.*, 2003, 3270-3277.
7. P. Šimon, R. Jambor, A. Růžička and L. Dostál, *J. Organomet. Chem.*, 2013, **740**, 98-103.
8. A. Luqman, V. L. Blair, R. Brammananth, P. K. Crellin, R. L. Coppel and P. C. Andrews, *Chem. Eur. J.*, 2014, **20**, 14362-14377.
9. M. Johnson, A. Bodi, L. Schulz and T. Gerber, *Nucl. Instrum. Methods Phys. Res. Sect. A-Accel. Spectrom. Dect. Assoc. Equip.*, 2009, **610**, 597-603.
10. B. Sztaray, K. Voronova, K. G. Torma, K. J. Covert, A. Bodi, P. Hemberger, T. Gerber and D. L. Osborn, *J. Chem. Phys.*, 2017, **147**, 013944.
11. D. W. Kohn, H. Clauberg and P. Chen, *Rev. Sci. Instrum.*, 1992, **63**, 4003-4005.
12. F. Neese, *WIREs Comput. Mol. Sci.*, 2012, **2**, 73-78.
13. F. Neese, *WIREs Comput. Mol. Sci.*, 2018, **8**, e1327.
14. E. v. Lenthe, E. J. Baerends and J. G. Snijders, *J. Chem. Phys.*, 1993, **99**, 4597-4610.
15. J.-D. Chai and M. Head-Gordon, *J. Chem. Phys.*, 2008, **128**, 084106.
16. S. Grimme, J. Antony, S. Ehrlich and H. Krieg, *J. Chem. Phys.*, 2010, **132**, 154104.
17. (*a*) D. A. Pantazis, X.-Y. Chen, C. R. Landis and F. Neese, *J. Chem. Theory Comput.*, 2008, **4**, 908-919; (*b*) D. A. Pantazis and F. Neese, *Theor. Chem. Acc.*, 2012, **131,** 1292.
18. C. Angeli, R. Cimiraglia, S. Evangelisti, T. Leininger and J.-P. Malrieu, *J. Chem. Phys.*, 2001, **114**, 10252-10264.
19. C. Angeli, R. Cimiraglia and J.-P. Malrieu, *Chem. Phys. Lett.*, 2001, **350**, 297-305.
20. C. Angeli, R. Cimiraglia and J.-P. Malrieu, *J. Chem. Phys.*, 2002, **117**, 9138-9153.
21. V. A. Mozhayskiy and A. I. Krylov, 2014.
22. S. Suzer, S. T. Lee and D. A. Shirley, *J. Chem. Phys.*, 1976, **65**, 412-417.
23. L. S. Wang, Y. T. Lee, D. A. Shirley, K. Balasubramanian and P. Feng, *J. Chem. Phys.*, 1990, **93**, 6310-6317.
24. G. Herzberg, *Molecular Spectra and Molecular Structure I: Spectra of Diatomic Molecules*, Krieger Publishing, Malabar, FL, 1989.
25. S. J. Blanksby and B. Ellison, *Acc. Chem. Res.*, 2003, **36**, 255-263.